This article has been accepted for publication in a future issue of this journal, but has not been fully edited. Content may change prior to final publication. Citation information: DOI 10.1109/LAWP.2021.3054863, IEEE Antennas and Wireless Propagation Letters

Low-cost, wideband checkerboard metasurfaces for monostatic RCS reduction

Akila Murugesan, *Student Member, IEEE*, Divya N, and Krishnasamy T. Selvan, *Senior Member, IEEE*

***Abstract*—This paper presents three wideband checkerboard metasurfaces (CMSs) for monostatic radar cross-section (RCS) reduction realized using low-cost FR4 material. The CMSs designed for the target RCS reduction of 10dB using the conventional phase deviation condition of 180±37°, when simulated, exhibit an overshoot in the lower frequency band and much higher reductions in the higher band. In order to maximize the bandwidth considering these variations, a constriction of 180±18° in the lower frequency band and a relaxation of 180±48° in the higher frequency band are made to the phase deviation condition. The three CMSs realized using these modifications offer a 10dB RCS reduction bandwidth over the range of 94-98%. The simulated and measured results compare favourably.**

***Index Terms*— Radar cross-sections, checkerboard metasurfaces, phase response, fractional bandwidth**

I. Introduction

The radar cross-section reduction (RCS) of flat metal targets realized using metasurfaces offers wideband performance. The checkerboard metasurface (CMS) is one type of metasurface used for RCS reduction based on the principle of destructive interference. The first work on CMS appeared in [1], which describes its construction by an artificial magnetic conductor (AMC) and a perfect electric conductor (PEC) arranged in a checkerboard fashion. Later, in [2], it was verified that an AMC-AMC pair provides broader bandwidth than an AMC-PEC pair. Subsequently, in [3-10], researchers contributed towards enhancing the 10dB RCS reduction bandwidth via suitable choices of elements for AMC construction. A phase deviation requirement of 180±37° between the two unit cells for an RCS reduction of 10dB was reported in [5], which employed a semi-empirical expression for RCS reduction using the reflection amplitudes and phases of the two AMCs. In [10], four different AMCs were used to construct the CMS in which the phase deviation of one pair of AMCs was stretched beyond 180±37°, while that of the other pair was maintained within 180±37°, thereby broadening the bandwidth. [11] explains how the 180±37° phase deviation results in 10dB RCS reduction using two sinusoidal signals. In [12], a semi-empirical expression for the RCS reduction was reported that considered AMCs with different echo areas and different reflection magnitudes. In [13], a multi-element metasurface featuring destructive interference was realized using an optimization-based approach, resulting in an extremely wide band. Although the bandwidth reported was very wide, the design and implementation complexity increased as elements of different heights were used, leading to the non-planarity of the metasurface. [14] reports a dual-band RCS reduction CMS with a transmission band in between.

Based on the literature, most of the research works have employed the Rogers substrate, which is a relatively expensive material. Hence, to reduce the CMS costs, a low-cost substrate FR4 was chosen for this work. Also, to the best of the authors' knowledge, FR4-based, extremely-wide bandwidth checkerboard metasurfaces have not been realized thus far. Among all the CMS studies, only [10] stretched the phase criterion beyond 180±37° to offer wideband, but the researchers used four AMCs rather than two to do so, resulting in a complex design. In this work, the authors propose an alteration to the phase deviation condition to enhance the bandwidth while limiting the number of AMCs to two. The modified criterion stretches the phase deviation to 180±48° in the upper-frequency band, while it shrinks it to 180±18° in the lower-frequency range. This phase modification introduced in the FR4-based CMS design to enhance the RCS reduction bandwidth is one of the novel contributions of this work. This work reports three CMSs with element pairs featuring single- and dual-resonant elements. Furthermore, the third CMS reported contains a novel pair comprising of a grounded dielectric slab and a novel slotted-cross element with 'L' corners. This combination of elements has not been reported so far.

Section II describes the proposed phase modification used to realize CMSs on FR4 substrates, while Section III explains the three pairs of elements designed using the modified criteria. Finally, Section IV provides a discussion on the simulated and measured results.

II. Modified Phase Deviation Criteria

The customary procedure in the design of a checkerboard metasurface over the frequency band of interest involves: (i) two unit cells with unity reflection magnitudes, and (ii) a phase deviation of 180±37° between these cells. The RCS reduction CMS essentially operates on the principle of destructive interference, which is caused by the reflected signals from two adjoining elements with an appropriately

The authors are with Sri Sivasubramaniya Nadar College of Engineering, Kalavakkam, Chennai, TamilNadu-603110, India. M. Akila is a Research Scholar in the Department of Electronics and Communication (e-mail: akilam@ssn.edu.in).

N. Divya is an undergraduate student (e-mail: divya17039@ece.ssn.edu.in) and Krishnasamy T. Selvan is a professor (e-mail: selvankt@ssn.edu.in) in the same department.

This article has been accepted for publication in a future issue of this journal, but has not been fully edited. Content may change prior to final publication. Citation information: DOI 10.1109/LAWP.2021.3054863, IEEE Antennas and Wireless Propagation Letters

maintained phase difference. As mentioned earlier, this aspect is explained in [11] using sinusoidal signals. Maintaining a constant reflection coefficient over the entire wideband using an FR4 substrate is difficult due to the frequency-dependant characteristics of the dielectric. The reflection coefficients of Jerusalem cross (JC)-based unit cell pairs using FR4 and Rogers substrates are shown in Fig. 1. As it can be observed, the FR4-based unit cells present varying reflection magnitudes as a function of frequency, which affects bandwidth performance. Based on a similar observation, in [15], a modified criterion for the reflectarray design was used to realize a wideband reflectarray on an FR4 substrate.

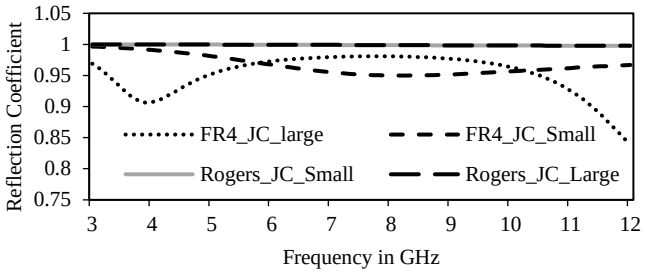

Fig. 1. The reflection coefficients of Jerusalem-cross-based unit cells (large-small) on FR4 and Rogers substrates.

The work started with the optimization-based design of CMS on an FR4 substrate, as per the configuration shown in Fig. 2, using the elements reported in [4]. The FR4-based Jerusalem cross (JC) structure, designed using the conventional phase deviation of 180±37°, provided the phase difference bandwidth over the range of 4.1 GHz to 10.5 GHz. After realizing the array, using the optimized dimensions, the simulated RCS reduction bandwidth was less than the phase difference bandwidth. The RCS reduction spiked to roughly -6dB around 4.7GHz, as shown in Fig. 3, thereby reducing the bandwidth. A similar overshoot of -8dB was reported in [4], which the authors attributed to the finite-size array. The authors of the present work believe that the overshoot is an effect of the mutual coupling and dielectric properties of the substrate. Further investigations into the impact of mutual coupling and substrate properties on the RCS reduction of checkerboard metasurfaces are recommended.

A few more CMS elements, which are not reported in this paper, were designed using optimization-based approach while considering the customary phase deviation approach. Upon realizing the CMS using the elements so designed, the RCS reduction bandwidth was consistently less than the phase difference bandwidth. The reduction in bandwidth was always due to the overshoots at the lower frequency. Simulation studies on different unit cell combinations always showed overshoots up to -6dB in the lower frequency band and greater reductions to about -15dB in the higher frequency band. Based on these observations concerning the operational bandwidth, the authors modified the phase deviation criteria for maximizing the bandwidth via optimization. The changes proposed include shrinking the phase deviation to 180±18° in the lower frequency band and broadening it to 180±48° in the higher frequency range.

The design procedure for producing a CMS on a high-loss, low-cost FR4 substrate using the modified phase deviation criteria can be summarized as follows: (i) choose a pair of elements, one single resonant, and the other dual resonant; (ii) define the transition frequency of the dual-resonant element as the mid-frequency between the lower- and upper-frequency bands; and (iii) optimize the elements' dimensions such that the phase deviation between the two elements is 180±18˚ in the lower frequency band and 180±48˚ in the upper-frequency band.

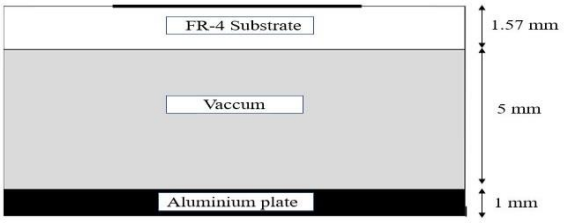

Fig. 2. Side view of the metasurface.

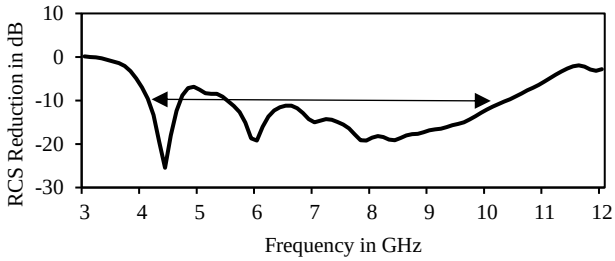

Fig. 3. RCS reduction of Jerusalem-cross-based CMS with a phase deviation of 180±37° on FR4 material.

III. ELEMENT DESIGN

The proposed modification to the phase deviation criteria was employed in the design of three different CMSs. The first two pairs of elements were chosen from [4] and [7], while the third pair is novel. The three structures are: i) a Jerusalem cross (JC) large-small pair, ii) a simple cross-slotted cross pair, and iii) a slotted cross with 'L' corners paired with a grounded dielectric slab. The designs utilized a 1.57 mm-thick FR4 substrate over an air gap of 5mm, a side view of which is shown in Fig. 2. The effective dielectric constant of the FR4-air gap combination was estimated using equation reported in [16] as follows:

$$\varepsilon_{eff} = \frac{d_1\varepsilon_{r1} + d_2\varepsilon_{r2}}{d_1 + d_2} \quad (1)$$

where d_1 and d_2 are the thicknesses and ε_{r1} and ε_{r2} are the permittivities of the two dielectric layers used. The equivalent dielectric constant estimate is1.67 over a height of 6.57 mm.

The first CMS uses two JCs of different dimensions, one large and the other small, as shown in Fig. 4. The second CMS uses a pair of elements that consist of a slotted cross element combined with a simple cross, as shown in Fig. 5. In the process of designing the first two structures, it was noted that one of the elements was large, while the other was small. Hence, the authors decided to create a third metasurface that combined a novel element with a grounded dielectric slab, as shown in Fig. 6. This novel element has a slotted cross in the centre with 'L'-shaped corners. Here, the 'L' structures were added at the four corners to enhance the bandwidth, as

This article has been accepted for publication in a future issue of this journal, but has not been fully edited. Content may change prior to final publication. Citation information: DOI 10.1109/LAWP.2021.3054863, IEEE Antennas and Wireless Propagation Letters

explained in [6]. The grounded dielectric slab acts as a single resonant element. This characteristic can be explained by estimating the surface impedance analytically, as reported in [17]. The analytical and simulated phase responses of the grounded dielectric slab are shown in Fig. 7.

All unit cells for the three configurations are 15mm×15mm in dimension. Table I provides the optimized dimensions for all three element pairs, and Fig. 8 shows the three fabricated prototypes.

IV. Results and Discussion

A. Phase Difference Bandwidth

The phase difference bandwidths of the reported structures are 99%, 97%, and 96%, respectively. The corresponding frequency ranges are 4.2-12.6 GHz for the Jerusalem cross pair, 4.1-11.6 GHz for the simple cross-slotted cross pair, and 4.1-11.7 GHz for the slotted cross with 'L' corners – grounded dielectric slab pair. The phase response of each pair of unit cells and their phase difference are shown in Fig. 9, 10 and 11.

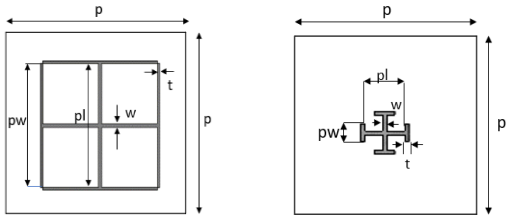

Fig. 4. (a) Jerusalem cross large, and b) Jerusalem cross small.

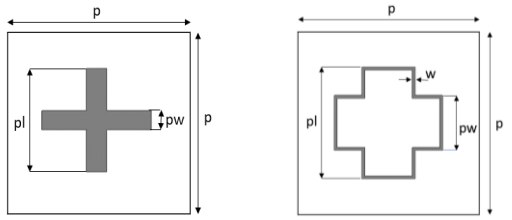

Fig. 5. a)Simple cross, and b)slotted cross.

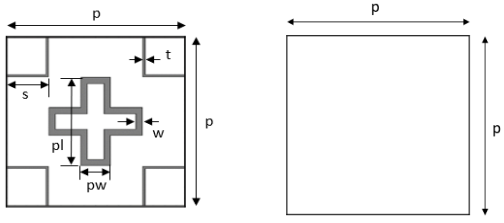

Fig. 6. a) Slotted cross with 'L' corners, and b) grounded dielectric slab.

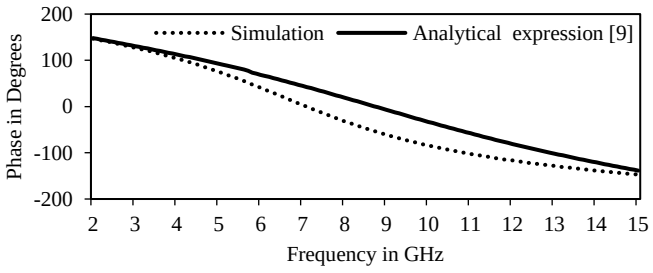

Fig. 7. Phased response of the grounded dielectric slab.

TABLE I

Dimensions of the Unit Cells in mm

Parameter	Structure 1		Structure 2		Structure 3	
	JC-Small	JC-Large	Simple cross	Slotted cross	Slotted cross with 'L' corners	No Element
p	15	15	15	15	15	15
pl	2	10.6	8.6	11.7	7.9	--
pw	1	10.6	1.6	5.7	2.5	--
w	0.2	0.3	--	0.6	1.1	--
t	0.2	0.2	--	--	0.2	--
s	--	--	--	--	3.5	--

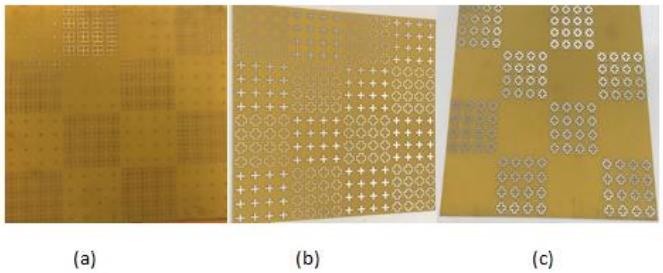

Fig. 8. a) Jerusalem cross large-small, b) simple cross-slotted cross, and c) slotted cross with 'L' corners – no element.

B. Simulated and Measured RCS Reductions

The checkerboard metasurface is 240mmx240mm, made of 4x4 AMCs, with each AMC consisting of 4x4 unit cells. The simulated structures are fabricated and measured. The measurements were performed at the facility available at the authors' institution in an outdoor setup. Maintaining a far-field separation of 7m between the horn antennas and metasurface-mounted absorber panel was not possible, as the power delivered from the antenna was too low. Hence, the two identical horn antennas connected to the network analyzer were placed 2m away from the metasurface-mounted absorber panel while measuring the RCS reduction. The simulated and measured results of the three structures are shown in Fig. 12, 13, and 14. The measurement results match those of the simulations well. The 10dB RCS reduction bandwidth values obtained through simulations and measurements are shown in Table II.

The simulated results are compared with the predicted results based on equation (19) in [12]. The predicted results show 8dB RCS reduction in the upper band, which deviates from the simulated output. This deviation could have occurred as the expression does not consider the factors such as mutual coupling, the frequency-dependent characteristics of the dielectric. A thorough investigation on which is recommended.

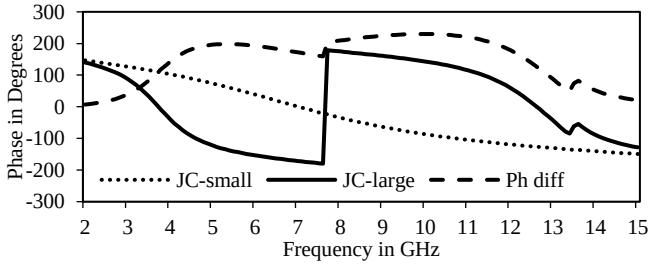

Fig. 9. Phase response of the Jerusalem cross large-small elements and the corresponding phase difference.

This article has been accepted for publication in a future issue of this journal, but has not been fully edited. Content may change prior to final publication. Citation information: DOI 10.1109/LAWP.2021.3054863, IEEE Antennas and Wireless Propagation Letters

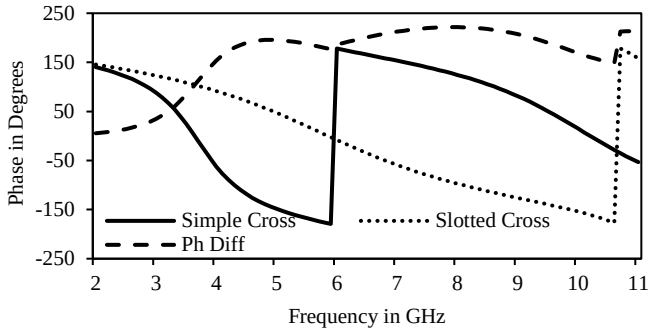

Fig. 10. Phase response of the simple cross-slotted cross pair and the corresponding phase difference.

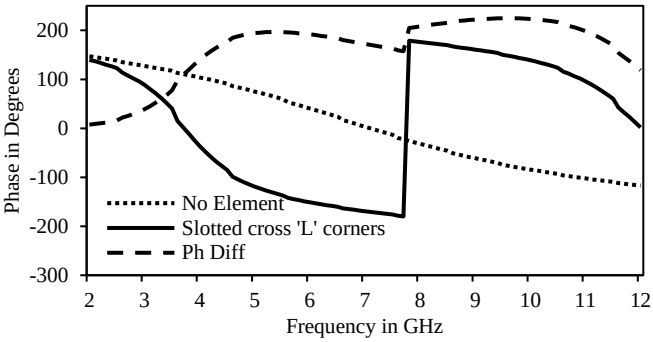

Fig. 11. Phase response of the slotted cross with 'L' corners – no element and the corresponding phase difference.

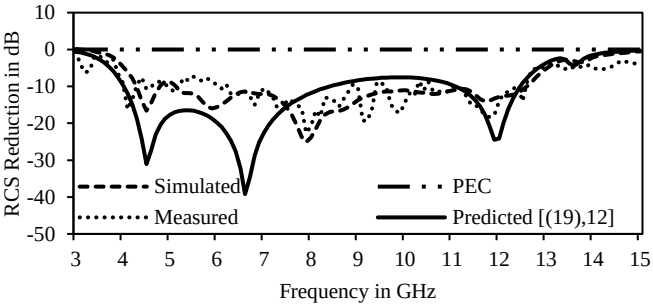

Fig. 12. Monostatic RCS reduction for the Jerusalem-cross-based CMS.

The measurement results show spikes up to -8dB at a few points. The reported fractional bandwidth includes these spikes. In the case of the Jerusalem cross structure, the 100% bandwidth includes a peak of -7.5dB at 5.5 GHz, as seen in Fig. 12. These spikes could be attributed to the measurement setup or the measurement being performed in an outdoor environment.

Table II shows the performance comparison with similar CMSs. For a fair comparison, we have chosen works that considered CMSs constructed using a pair of unit cells with a phase deviation of 180±37° realized on single-layer substrates with or without an air gap.

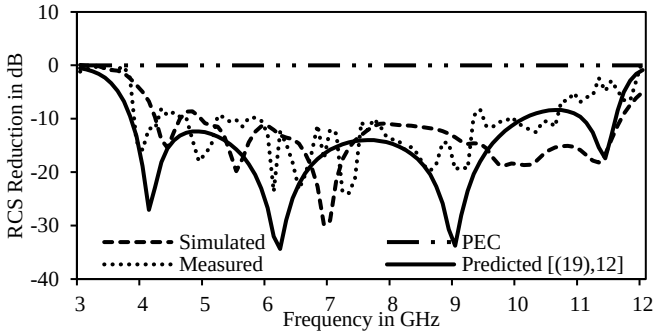

Fig. 13. Monostatic RCS reduction for the simple cross-slotted cross based CMS

.

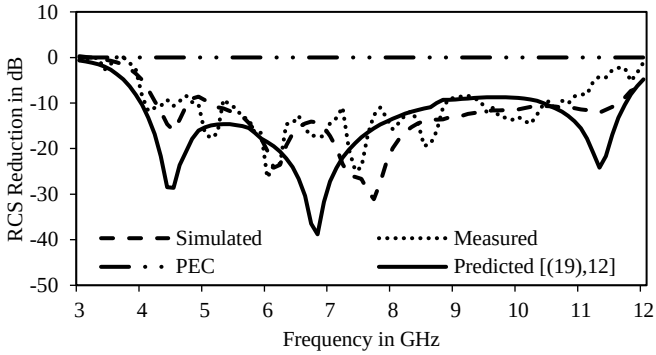

Fig. 14. Monostatic RCS reduction for the slotted cross with 'L' corners and grounded dielectric slab based CMS.

V. Conclusion

Three extremely wideband CMSs were designed for a 10dB RCS reduction using high-loss, low-cost FR4 material. The CMSs were initially designed using the customary condition of 180±37° for an RCS reduction of 10dB. The simulated response showed an overshoot in the lower-frequency band and a greater reduction in the higher frequency band. To enhance the bandwidth based on these observations, the phase deviation was tightened to 180±18° in the lower frequency band and stretched to 180±48° in the higher frequency band. The three CMSs designed using these modified conditions offer 10dB RCS reduction bandwidths of 98%, 94% and 94% over the frequency ranges 4.3 to 12.6 GHz, 4.2 to 11.7 GHz and 4.2 to 11.6 GHz, respectively. The measurements compare favourably with the simulation results.

TABLE II

COMPARSON WITH SIMILAR WORKS

Ref. /Year	Height of substrate in mm (Substrate used)	ε_r/ ε_{eff}		-10 dB RCS reduction band in GHz (fractional bandwidth)	
				Simulated	Measured
[3] / 2015	6.35(Rogers5880)	2.2		4.2-7.9 (61%)	4.2-7.8 (60%)
[4] / 2016	6.35(Rogers5880)	2.2		3.94-7.4 (61%) 8.41-10.72 (24%)	3.94-7.4 (61%) 8.41-10.72 (24%)
[5] / 2017	6.35(Rogers5880)	2.2		3.75-10 (91%)	3.75-10 (91%)
[6] / 2019	11(vacuum) + 0.5 (Rogers RO4350B)	3.48/1.1		3.78-10.08 (90.9%)	3.77-10.14 (91.5%)
[7] / 2019	3.175(TaconicTLY5)	2.2		8-16 (66.7%)	7.98-16.32 (68.6%)
This work	5 (vacuum) +1.57 (FR4)	4.3/1.67	(i)	4.3-12.6 (98%)	4.1-12.3 (100%)
			(ii)	4.2-11.7 (94%)	3.9-10.6 (92%)
			(iii)	4.2-11.6 (94%)	4.1-10.9 (91%)

VI. REFERENCES

[1] M. Paquay, J. Iriarte, I. Ederra, R. Gonzalo, and P. de Maagt, "Thin AMC Structure for Radar Cross-Section Reduction," *IEEE Transactions on Antennas and Propagation*, vol. 55, no. 12, pp. 3630-3638, Dec. 2007, doi: 10.1109/TAP.2007.910306.

[2] M. E. de Cos, Y. Alvarez-Lopez, and F. Las Heras Andres, "A Novel Approach for RCS Reduction Using a Combination of Artificial Magnetic Conductors," *Progress In Electromagnetics Research*, vol. 107, pp. 147-159, 2010.

[3] Y Fu, Y Li, and N Yuan, "Wideband Composite AMC Surfaces for RCS Reduction," *Microwave and Optical Technology Letters*, vol. 53, no. 4, pp. 712-715, Apr 2011.

[4] J. C. Iriarte Galarregui, A. Tellechea Pereda, J. L. M. de Falcón, I. Ederra, R. Gonzalo, and P. de Maagt, "Broadband Radar Cross-Section Reduction Using AMC Technology," *IEEE Transactions on Antennas and Propagation*, vol. 61, no. 12, pp. 6136-6143, Dec. 2013, doi: 10.1109/TAP.2013.2282915.

[5] W. Chen, C. A. Balanis, and C. R. Birtcher, "Checkerboard EBG Surfaces for Wideband Radar Cross Section Reduction," *IEEE Transactions on Antennas and Propagation*, vol. 63, no. 6, pp. 2636-2645, June 2015, doi: 10.1109/TAP.2015.2414440.

[6] W Chen, C A. Balanis, and C R. Birtcher, "Dual Wide-Band Checkerboard Surfaces for Radar Cross Section Reduction," *IEEE Transactions on Antennas and Propagatio*n, vol. 64, no. 9, pp. 4133-4138, Sept 2016.

[7] V. A. Libi Mol, and C. K. Aanandan, "Wideband Radar Cross Section Reduction Using Artificial Magnetic Conductor Checkerboard Surface," *Progress In Electromagnetics Research M*, vol. 69, pp. 171–183, 2018.

[8] D. Sang, Q. Chen, L. Ding, M. Guo, and Y. Fu, "Design of Checkerboard AMC Structure for Wideband RCS Reduction," *IEEE Transactions on Antennas and Propagation*, vol. 67, no. 4, pp. 2604-2612, Apr 2019

[9] S. H. Kim, and Y. J. Yoon, "Wideband Radar Cross-Section Reduction on Checkerboard Metasurfaces With Surface Wave Suppression," *IEEE Antennas and Wireless Propagation Letters*, vol. 18, no. 5, pp. 896-900, May 2019, doi: 10.1109/LAWP.2019.2905012

[10] A. Y. Modi, C. A. Balanis, C. R. Birtcher, and H. N. Shaman, "Novel Design of Ultrabroadband Radar Cross Section Reduction Surfaces Using Artificial Magnetic Conductors," *IEEE Transactions on Antennas and Propagation*, vol. 65, no. 10, pp. 5406-5417, Oct. 2017, doi: 10.1109/TAP.2017.2734069.

[11] A. Murugesan, and K. T. Selvan, "On Further Enhancing the Bandwidth of Wideband RCS Reduction Metasurfaces Using an Optimization Algorithm," Submitted to *International Journal of RF and Microwave Computer aided Engineering.*

[12] A. Y. Modi, C. A. Balanis, C. R. Birtcher, and H. N. Shaman, "New Class of RCS-Reduction Metasurfaces Based on Scattering Cancellation Using Array Theory, " *IEEE Transactions on Antennas and Propagation*, vol. 67, no. 1, pp. 298-308, Jan. 2019, doi: 10.1109/TAP.2018.2878641.

[13] J. Su, Y. Lu, J. Liu, Y. Yang, Z. Li, and J. Song, "A Novel Checkerboard Metasurface Based on Optimized Multielement Phase Cancellation for Superwideband RCS Reduction," *IEEE Transactions on Antennas and Propagation*, vol. 66, no. 12, pp. 7091-7099, Dec. 2018, doi: 10.1109/TAP.2018.2870372.

[14] Y. Pang *et al*., "Wideband RCS Reduction Metasurface with a Transmission Window," *IEEE Transactions on Antennas and Propagation*, vol. 68, no. 10, pp. 7079-7087, Oct. 2020, doi: 10.1109/TAP.2020.2995429

[15] J. Ethier, M. R. Chaharmir, J. Shaker, and D. Lee, "Development of Novel Low-Cost Reflectarrays [Antenna Applications Corner]," *IEEE Antennas and Propagation Magazine*, vol. 54, no. 3, pp. 277-287, June 2012, doi: 10.1109/MAP.2012.6294005.

[16] F. Costa, A. Monorchio, and G. Manara, "Efficient Analysis of Frequency-Selective Surfaces by a Simple Equivalent-Circuit Model," *IEEE Antennas and Propagation Magazine*, vol. 54, no. 4, pp. 35-48, Aug. 2012, doi: 10.1109/MAP.2012.6309153

[17] M. Fallah, F. H. Kashani, and S. H. Mohseni Armaki, "A Novel and Simple Analytical Method for Analysis of AMC and EBG Properties of Lossless Artificial Impedance Surfaces," *Progress In Electromagnetics Research Symposium Proceedings*, Marrakesh, Morocco, Mar. 20–23, 2011.